C60-small arylamine push-pull dyads for single-material organic solar cells

Andreea Petrolela Diac, Lorant Szolga, Clément Cabanetos, Alexandra Bogdan, Anamaria Terec, Ion Grosu, Jean Roncali

Parameters Influencing Fatigue Life Prediction of Dielectric Elastomer Generators

C. Jean-Mistral[1*], G. Jacquet-Richardet[1], A. Sylvestre[2]
[1]Univ Lyon, INSA-Lyon, CNRS, UMR5259, LaMCoS, F-69621, France
[2] Univ. Grenoble Alpes, CNRS, Grenoble INP, G2Elab, F-38000 Grenoble, France
[*]Corresponding author. E-mail address: Claire.jean-mistral@insa-lyon.fr

Abstract: For energy scavenging applications, estimating fatigue life of dielectric elastomer is as crucial as computing the amount of scavenged energy. Crack growth approach, well known in rubber industry, is a fast methodology to estimate fatigue life. We adapt this methodology to dielectric silicone elastomers (Elastosil 2030) and we focus in particular on the factors influencing this estimation such as sample geometry, tearing energy, power law. We underline that the variation in tearing energy estimation induces a small dispersion on the fatigue life estimation whereas power law identification is the crucial and critical parameter. Finally, we define an index of performance based on fatigue life and scavenged energy density, and we compare two materials (acrylic 3MVHB4910 and silicone Elastosil 2030).

Keywords : Dielectric Elastomer, Fatigue life, Crack growth approach, Energy scavenging

1. Introduction

For energy scavenging applications involving human or fluid interaction (water, wind), Dielectric Elastomer Generators (DEGs) **[1-6]** are promising soft electrostatic candidates due to their lightweight, low cost and high scavenged energy density (0.834 $J.g^{-1}$) **[7]**. Pelrine, firstly described in 2001 a DEG embedded in a shoe able to scavenge 0.8J per step under a poling voltage of 2.5kV **[1]**. In 2008, Jean-Mistral *et al.* have developed a scavenger located behind the knee, able to scavenge 100µW under low poling voltage (170V) and moderate strain (50%) during classic walk and up to 1.74mW under high poling voltage (1000V) **[3]**. More recently, Vu Cong *et al.* developed an hybrid structure mixing electret and dielectric that can scavenge up to 33µW under a strain of 50% at 1Hz **[4]**. For human kinetic scavenging energy, several hybrid structures were proposed since this first, to remove the needed poling voltage of DEGs, most of them combining electret or piezoelectric with dielectric elastomers **[4-5].** Regarding large-scale applications, above the buoys initially developed, the SBM company designed since 2012 a multi-modal wave tube in dielectric elastomer as wave energy converter **[2]** and Fontana and Vertechy proposed ocean water columns with DEGs. Both of these two projects scavenge few Watts and are currently in the real sea-test phase **[6]**. Among all the possible materials such as acrylic, natural rubber, polyurethane, silicone elastomers are one of the most interesting polymers due to their high energy density and low viscous losses **[8-9]**. Various theoretical and experimental modelling have been proposed to estimate the performances of DEGs in term of scavenged energy density and efficiency **[10-11]**, but most of the time without taking into account the fatigue of the dielectric elastomers (DEs) which constitutes a crucial parameter to qualify this technology for real engineering applications. In 2015, Zhou *et al.* firstly introduced fatigue failure mode under cyclic loading in theoretical model, underlying that higher fatigue life leads to lower efficiency of DEG **[12]**. They underlined that choosing an appropriate polarization voltage improves the efficiency of the DEG without reducing the fatigue life. In 2018, these authors proposed a criterion to estimate fatigue life of elastomer under electromechanical loads **[13]**. From a dynamic point of view, fatigue life is usually determined from classic Wöhler curves (Stress-Number of cycles, S-N). Lifetime under cyclic electromechanical loading in actuator mode has recently been carried out, underlying millions of potential operating cycles **[14-15]**. Nevertheless, as these S-N experiments remain long, a crack growth approach was proposed to estimate the fatigue life through simple and quick tests **[16-17]**. Firstly implemented for rubbers early in the 60's **[18]**, this approach has been improved, adapted to multi-axial loading **[19]** and recently successfully tested on DE material. In 2017, Fan *et al.* **[20]** studied the crack growth in an acrylic DE: an experimental protocol established

the power-law relation between the crack growth rate *da/dN* and the energy release rate *T*, thus predicting the fatigue life of acrylic VHB4910 with an edge crack of 1 mm. From this approach, no studies have been developed for silicone elastomers used as active materials in DEG applications and especially no research work on the factors influencing this fatigue life estimation. In this paper, we have used for the first time the crack growth approach to estimate the fatigue life of silicone in general, namely without pre-cut. Parameters affecting the estimation of this fatigue life have been highlighted with a focus on the sample geometry (pure shear or edge) and the mechanical parameters (tearing energy, elastic energy). Finally, a performance index *PI* is proposed to compare materials for energy scavenging applications and a comparison between acrylic 3M VHB 4910 and silicone Elastosil 2030 is conducted.

2. Experiments

Pure shear cut specimens of Elastosil 2030 from Wacker were prepared with the dimensions reported in Fig. 1. The initial thickness of the silicone is 160 µm. A ratio of ten between the initial length L_0 and the initial height h_0 insures to minimize edge effect, as seen in Fig.1, validating the pure shear test configuration. The initial length of the pre-cut is 25mm. The samples were glued onto plastic rigid frames to avoid any sliding into the jaws of the tensile set-up used (Lloyd 1 kN). As the silicone Elastosil 2030 is transparent, a chalk powder is deposited onto the surface to accentuate the contrast. Cycling loading/unloading tests between two limits ($\lambda_{min}=0$ and λ_{max}) were performed up to the complete mechanical rupture of the sample, at a strain rate of 5 mm.min^{-1} (Fig. 1(c). Tests were realized at ambient temperature (25°C). The maximal stretch ratio λ_{max} ($\lambda_{max} = h_{max}/h_0$ with h the height of the pure shear sample) varies from 1.1 to 1.5 with a step of 0.05, leading to an increase in the maximum tearing energy *T* (also named energy release rate) . Force was recorded using a 100 N force sensor and a 4 MPx camera took pictures every second. A post-treatment software computed the variation of the cut length $\Delta a=a_j-a_i$ between the ith and jth cycles which increases quite linearly with the increasing number of cycles (Fig.1). An average crack growth rate *da/dN* is then computed over 10 cycles. For each maximum stretch ratio λ_{max}, the experiments are at least reproduced on 6 different samples. The dispersion and measurement error are less than 12%.

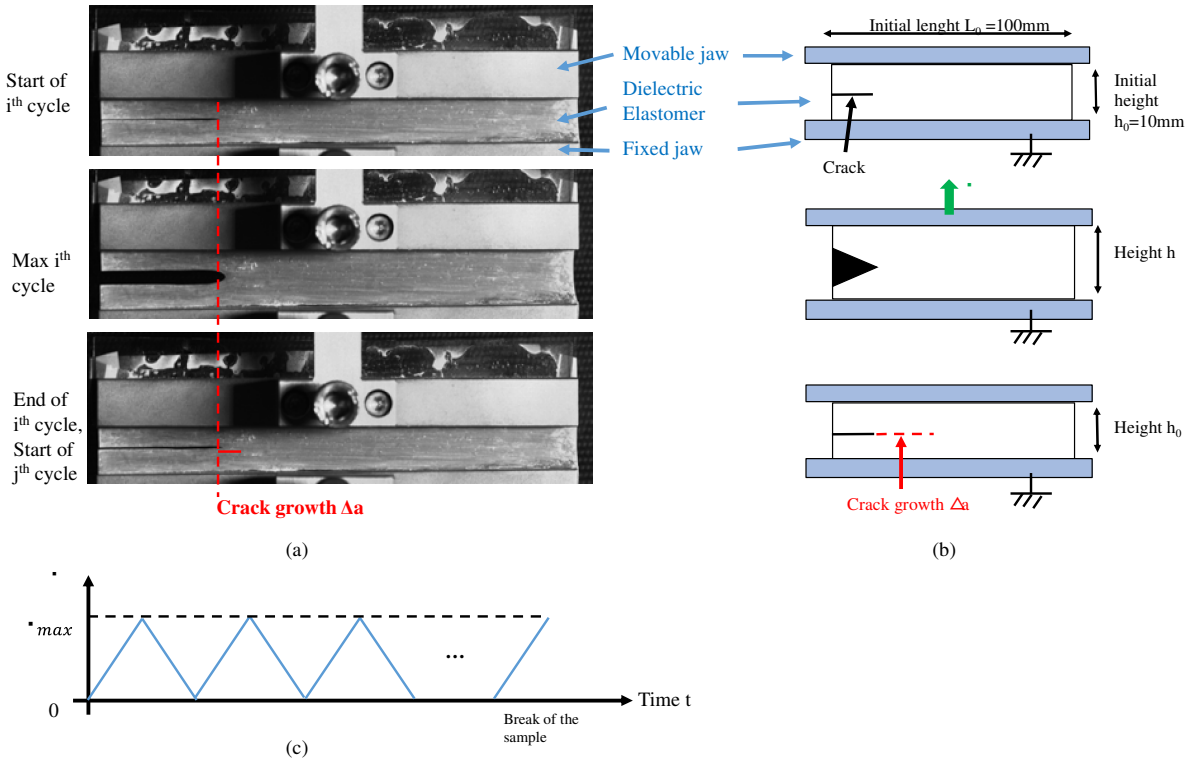

Figure 1: (a) Experimental pictures describing a cycle, (b) Schematics of the sample subject to cyclic loading-unloading with the visualization of the crack growth Δa, (c) Cyclic loading-unloading test

The crack grow rate da/dN is typically linked to the tearing energy T by assuming a simple power-law behavior **[16-21]**:

$$\frac{da}{dN} \tag{1}$$

with B and F the material parameters extracted from curve fitting between experiments and power-law modelling. The energy release rate is the change in the stored mechanical energy dU, per unit change in crack surface area dA, and it is a material intrinsic property **[21]**.

Pure shear and edge configurations were investigated in our study (Fig. 2). For the pure shear specimen (Fig.2, the tearing energy T_{pure} develops a simple expression:

$$T_{pure} \tag{2}$$

with h the height of the sample reported in Fig.1 and W_0 the strain energy density of a pristine sample (without cut) under a given applied stretch ratio λ_{max} recorded in steady-state in order to avoid Mullin's effect, namely for the Elastosil 2030 after five cycles.

The tearing energy T_{edge} associated to the edge configuration is:

$$T_{edge} = 2 * k * W_0 \tag{3}$$

with a the size of the crack and k a strain-dependent parameter defined by the expression given in Eq.4 **[22]** .

$$k = \frac{2.95 - 0.08\varepsilon}{} \tag{4}$$

where ε is the strain expressed as $\varepsilon = \lambda - 1$ with λ the strain ratio defined as the ratio between the final length L_1 and the initial length L_{10} : $\lambda_1 = L_1/L_{10}$.

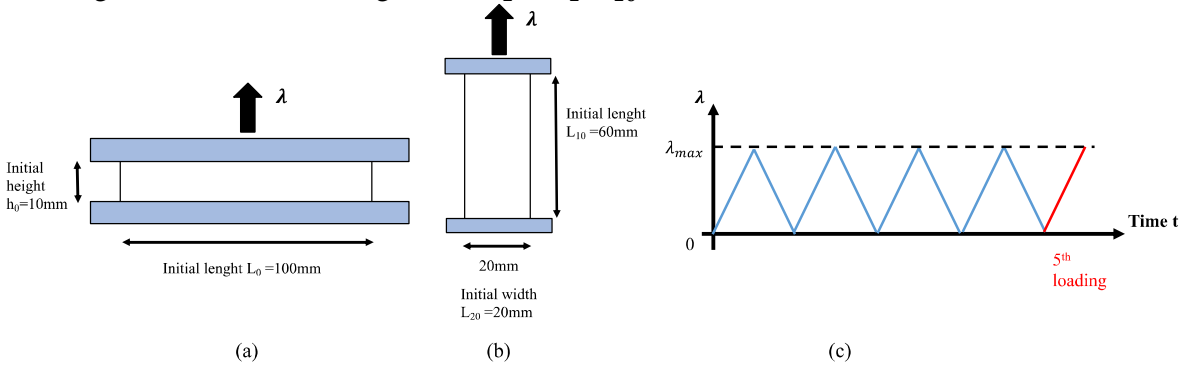

Figure 2: (a) Schematic of the pure shear configuration, (b) Schematic of edge configuration, (c) Cyclic loading-unloading test

Stress-Strain curves for the pristine silicone Elastosil 2030 are reported on Fig. 3 for pure shear (Fig. 3 (a)) and edge (Fig. 3 (b)) configurations. Cycling loading/unloading between two limits ($\lambda_{min}=0$ and $\lambda_{max}=1.5$) were also performed at a strain rate of 5 mm.min^{-1} and only the 5th loading is reported in Fig.3.

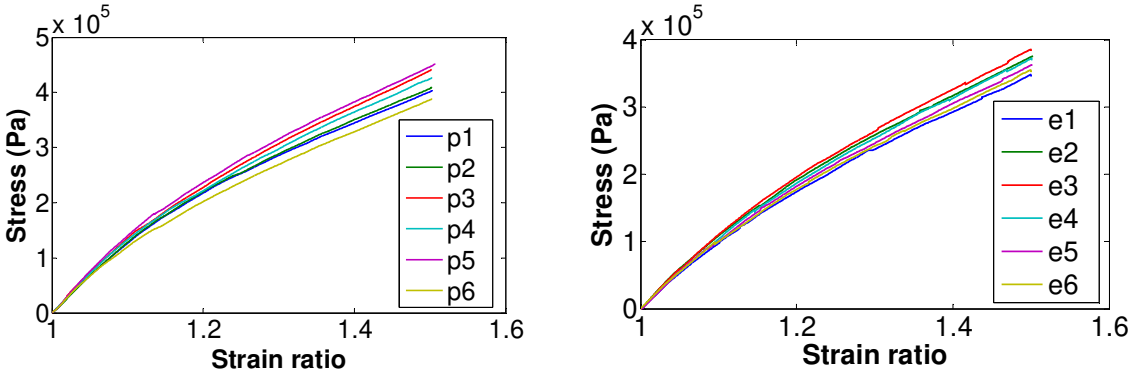

Figure 3: Stress-Strain curves for the silicone Elastosil 2030 obtained in (a) pure shear and (b) edge configurations for six different samples under an applied strain of 50%.

The value of the tearing energy T is controlled by adjusting the value of the maximal stretch ratio λ_{max} applied to the polymer. The tearing energy T for an imposed strain of 50% is about 476 J.m^{-2} for pure shear specimen (Eq. 2 and median curve) and about 374 J.m^{-2} for edge specimen (Eq.3 and median curve), values in agreement with literature **[20, 22-23]**. In 2012, Pharr *et al.* **[22]** carried out rupture experiments (one loading) on pristine and pre-cut acrylic 3MVHB4905 samples. They found that the fracture energy, independent of the sample geometry, increases with the stretch-rate (from 1500 J.m^{-2} to 5000 J.m^{-2} for a stretch rate of 1/min and 100/min respectively) while the stretch at rupture decreases with sample height. Fan *et al.* underlined a maximum tearing energy varying from 0.212 kJ.m^{-2} up to 3.10 kJ.m^{-2} for maximum stretches of 1.5 and 4.5 respectively **[20]**. Kaltseis *et al.* confirmed the value of fracture energy **[23]** and they show that it is almost double for natural rubber compared to acrylic rubber at a strain rate of 100%/s. In theory, our values should be independent of the stretching mode as the tearing energy T is a material property but, as seen practically it is not the case. Even if they remain close and comparable (476 J.m^{-2} with pure shear and 374 J.m^{-2} with edge configuration) with the one reported in literature, this difference can affect significantly the estimation of the fatigue life. Thus, estimation of fatigue life will be computed in both case: pure shear and edge configurations.

3. Results and discussions

3.1 Fatigue life estimation

From the crack growth propagation tests described in section 2 and Fig.1, the crack growth rate *da/dN* can be computed as the average of the crack growth Δa over 10 cycles. The tearing energy T is extracted from classic "Stress-Strain" curves on pristine sample in pure shear mode (Fig.3a), as the tearing energy T is varying through controlling the maximal stretch λ_{max}. Thus, the power-law describing the relationship between the crack growth rate da/dN and the tearing energy T can be deduced from Fig. 4.

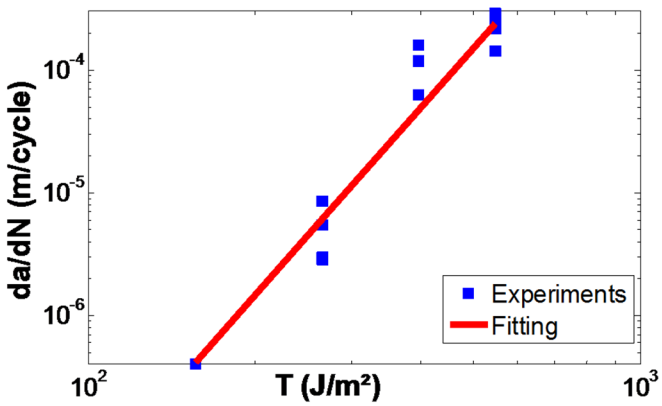

Figure 4: Crack growth rate *da/dN* as a function of tearing energy T

For the silicone Elastosil 2030, the two fitted parameters extracted from Eq.1 are B=2.65 10^{-18} (m/cycles)/(J/m²) and F=5.1, in agreement with literature where F usually varies between 2 and 6 and B can drastically change **[20, 24-26]**. Table 1 summarizes the parameters B and F for various rubbers.

Table 1: Parameters B and F for various rubbers

	Natural Rubber (NR)	Polybutadiene (BR)	NR filled with 31% of carbon black and 9.5% plasticizer (NR CB21)	NR Filled with 23% carbon black (NR CB23)	3M VHB 4910	Elastosil 2030
	Mars[24]	Mars[24]	Zarrrin[25]	Papadopoulos[26]	Fan[20]	This work
B (m/cycles)/(J/m2)	4.46 10^{-12}	12 10^{-18}	4 10^{-14}	1.36 10^{-11}	3.95 10^{-10}	2.65 10^{-18}
F	1.35	3.44	2	1.93	4.43	5.1

In order to improve accuracy in the determination of this power law, the crack growth rate da/dN as a function of the tearing energy T is plotted only for value of λ_{max} varying between 1.15 and 1.3. Indeed, for low value of λ_{max} (λ_{max} =1) namely low value of the tearing energy T, the quantity da/dN seems mis-estimated as the length of the crack Δa is in the same order of magnitude of the pixel of the image recorded by the camera. At the opposite, for high values of λ_{max} (λ_{max} >1.3) namely high value of tearing energy T, a scamera with an higher speed (>4MPx) is necessary to properly define da/dN as the crack propagation remains quite fast. One can also note that for extreme value of stretch (λ_{max} =1.5), the samples were broken in only one cycle. Thus, lower and higher values of tearing energy T cannot be considered as reliable and suitable for our power-law fitting. Finally, for each test configuration namely for each maximal stretch λ_{max} , six tests were conducted as described in section 2 and we reported in Fig. 4 only the relevant one, namely the ones with quite horizontal crack propagation, with no defect or sudden change of behavior. This selection leads to post-treat three to four measurements for each configuration. Thank to this careful choice of measurements, the power-law fitting remains quite correct with a coefficient of determination R^2 equal to 0.85. Including all the measurements drastically decreases the accuracy of the fitting (R^2=0.61). Fatigue life N_f is finally determined by integrating the growth rate da/dN of a pre-existing small flaw growing from its initial size a_0 up to its critical size a_f:

$$N_f = \int_0^{N_f} dN = \int_{a_0}^{a_f} \frac{da}{dN} \tag{5}$$

By combining Eq.1 and Eq.5, the fatigue life N_f can be expressed as:

$$N_f = \int_{a_0}^{a_f} \frac{1}{BT^F} da \tag{6}$$

According to Mars and Fatemi **[18]**, this analysis is only valid for small cracks hypothesis and edge crack specimens, namely when tearing energy can be written as a product of strain energy density W_0 and crack size a (combining Eq.3 and Eq. 6). We also opted to implement this theory for pure shear specimen (combining Eq.2 and Eq. 6). Two expressions of fatigue life, one for pure shear specimen $N_{f,pureshear}$ and one for edge crack specimen $N_{f,edge}$, are deduced and used to estimate the fatigue life of dielectric elastomer:

$$N_{f,pureshear} = \frac{1}{BT^F}[a_f \tag{7}$$

$$N_{f,edge} \quad 1 \quad 1 \quad 1 \tag{8}$$

where a_0 represents the flaw size into the elastomer.

Classically, the crack growth approach is used to determine the fatigue life of sample with an initial pre-cut. Here, we applied this methodology to pristine sample with an initial internal defect, leading to an estimation of mechanical fatigue life in general, i.e. a prediction of the fatigue life of the material. According to **[18]**, a_0 and can vary from 20.10^{-6} m up to 50.10^{-6} m. The smaller value of 20 µm is chosen for our calculations leading to the maximal value of fatigue life.

Fig. 5 shows the estimation of fatigue life $N_{f,edge}$ of the silicone Elastosil 2030 (blue solid line) in edge configuration (Eq. 3 and Eq. 8) with our experimental parameters (B, F and T). The crucial parameters influencing this estimation are highlighted in Fig. 5 such as the choice of the configuration ($N_{f,pureshear}$) or the choice of the material parameters ($N_{f,3MVHB4910}$, $N_{f,NR,}$ $N_{f,NR\ CB21}$, $N_{f,NR\ CB23}$ and $N_{f,BR}$). Indeed, the green solid line in Fig. 5 is also the estimation of the fatigue life $N_{f,pureshear}$ of the silicone Elastosil 2030 but computed in a pure shear configuration, namely using Eq. 2 and Eq. 7. The dash lines in Fig. 5 represent the estimation of the fatigue life of the silicone Elastosil 2030 in edge configuration (Eq. 3 and Eq. 8) but with material parameters from literature (Table 1).

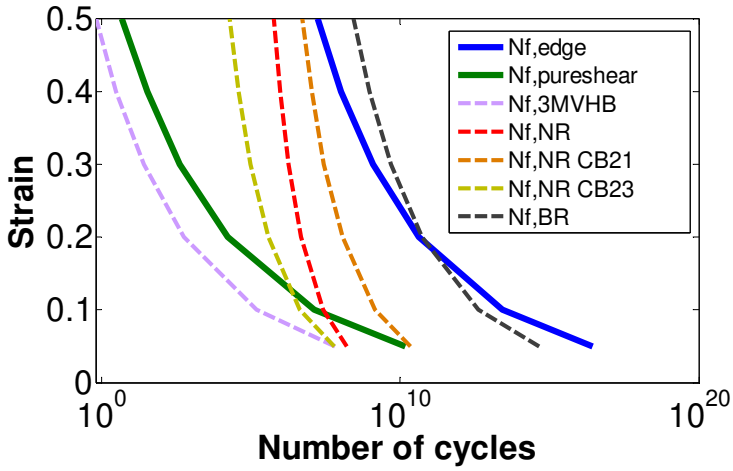

Figure 5: Estimation of the fatigue life of the silicone Elastosil 2030 in pure shear $N_{f,pureshear}$ and edge $N_{f,edge}$ configurations with parameters B and F from Table 1.

The more the applied strain increases, the more the fatigue life of the DE decreases (Fig. 5), as classically observed for Wöhler curves. Using our experimental material parameters B and F, 1.5 10^{10} cycles could be achievable with the pure shear estimation ($N_{f,pureshear}$ in Fig. 5) and up to 2.8 10^{16} cycles for edge crack estimation ($N_{f,edge}$ in Fig. 5) under an applied strain of 5 %. Under 50 % of applied strain, 5 cycles and 17.3 millions of cycles are respectively predicted. The difference observed between these two estimations of fatigue life for a given applied strain, remains quite important: a factor of 10^6. Nevertheless, if material parameters from literature (NR CB21 from Table 1) are used instead of ours, the estimation of fatigue life for the silicone Elastosil 2030 in edge configuration (2.8 10^{10} cycles) and in pure shear configuration (1.42 10^9 cycles) for an applied strain of 5 %, are quite similar (Eq. 7 and Eq. 8). The difference observed between the two estimations with our parameters, is therefore more a consequence of the material parameters B and F rather than to the model chosen and its associated configuration (Eq. 7 or 8). On another end, a fatigue life of zero is predicted for the silicone Elastosil 2030 under 50 % of strain, if the material parameters B and F of the 3MVHB polymer are used ($N_{f,3MVHB4910}$ in Fig. 4). An over-estimation in the fatigue life of Elastosil 2030 under 50 % of strain, is done with material parameters of polybutadiene ($N_{f,BR}$ in Fig.4): prediction of 277 millions of cycles. Thus, material parameters B and F must be determined carefully and edge configuration (Eq.8) will be used to estimate the fatigue life as the predictions obtained with this modelling appear more realistic in a majority of cases.

One can also remind that in theory the strain energy density W_0 and the tearing energy T are intrinsic material parameters and must not vary with the geometry of the specimen. This assumption is inaccurate in experiments (Fig. 3) and will lead to the definition of a range for the estimation of the fatigue life (min/max). As an example, if the two extreme Stress-Strain curves are used instead of the

median one (Fig. 3), the predictions of the fatigue life $N_{f,edge}$ of the silicone Elastosil 2030 under 50 % are respectively 21.1 millions of cycles and 12.1 millions of cycles instead of 17.3 millions of cycle with the median value. The dispersion on the prediction of fatigue life remains reasonable (<30 %) which justifies the use of the median Stress-Strain curve as reference for the estimation of the fatigue life.

Our results clearly underline that crack growth approach could be used for dielectric elastomer with a life estimation based on edge crack configuration (Eq.8). Our original analysis underlines that the power laws have a tremendous impact on the estimation of fatigue life and that the mechanical quantities (tearing energy and elastic energy) have less influence and lead to the definition of a range for the estimation of the fatigue life. This test method is clearly time-saving compared to S-N tests as it can give a prediction of the fatigue life of DE in few days instead of months even years for classic fatigue tests. In transducer applications especially in scavenging applications, this estimation of fatigue life is crucial for the development and widespreading of the technology. Researchers, scientists and engineers need a trustful test methodology to quickly estimate the life time of their structures. Crack growth method can be the solution. Nevertheless, our estimation of fatigue life for pristine sample based on crack growth approach must be compared to classic S-N tests to valid this quick methodology, to verify that no over or under-estimations are realized and to extend it to electromechanical loading. Thus, a classic S-N test set-up have been developed in our laboratory and classic S-N tests are running.

Finally, in Fig. 5, the estimation of the fatigue life $N_{f,edge}$ for the Elastosil 2030 is done for a given range of strain (10-50 %). A Basquin model (Eq. 9) could be used to describe our estimation of fatigue life in the 10-50 % strain range, and can also be used to predict the fatigue life for higher strain. This 1D model generally describes the experimental data obtained from classic S-N test.

$$NS^m = C \tag{9}$$

with N the number of cycles, S the strain. m and C are two material parameters found by fitting between the analytical equation (Eq.9) and the fatigue life data (Fig.4). With our data, m=9.2 and C=2.16 10^4, in agreement with awaited values (1/m is generally closed to 0.1, and C can have very different value).

3.2 Comparison of DE for energy scavenging applications

In the field of dielectric elastomer generators, materials are generally chosen only in function of the energy that they can scavenge. More energy they can scavenge and more they are well-suited for generator applications, even if they can realize only few cycles. Nevertheless, for most of the energy scavenging applications, millions of cycles are required. In **[2],** a fatigue life of 20 millions of cycles is defined as a minimum. An index of performances combining the value of scavenged energy and the predicted fatigue life must be defined to compare various polymers for energy scavenging applications. Thus, in this paper, we define such an index of performances *PI* which clearly was required by the community.

The maximum energy density scavenged by a dielectric elastomer can be predicted from the maximum operating area, which is limited by the failures occurring into the polymer **[10]**. This maximum theoretical energy density is computed in a biaxial mode as in this basic configuration, dielectric elastomer scavenges more energy than in a uniaxial or pure shear modes. This energy density is estimated using our thermodynamic modelling as described in **[7]**, without taking into account the possible variations of the dielectric constant and the electrical breakdown with strain. Viscous losses occurring into the dielectric elastomer are neglected as they remains very low in silicone elastomer. A Yeoh hyperelastic modelling is classically used for silicone elastomer with the true stresses T_i written as:

$$T_i = \lambda_i \frac{\partial W}{\partial \lambda_i} - p \tag{10}$$

λ_i is the extension coefficient on the axes (L_1 stands for the lenght, L_2 for the height, L_3 for the thickness of the silicone), W is the strain energy and p the hydrostatic pressure. This pressure is unknown and depends on the boundary conditions of the mechanical structure. The Yeoh strain energy W is given by equation 11:

$$W = C_{10}(I_1 - 3) + C_{20}(I_1 - 3)^2 + C_{30}(I_1 - 3)^3 \tag{11}$$

with I_1 is the first invariant $I_1 = \lambda_1^2 + \lambda_2^2 + \lambda_3^2$ of the left Cauchy Green deformation tensor. The C_{ij} parameters describe the hyper-elastic response and it is calculated by fitting the model (Eq. 9 and 10) to a uniaxial tensile test (Fig. 3). In our case, the fitted parameters are C_{10}=0.3358 MPa, C_{20}=0.1675 MPa and C_{30}=0.07291 MPa.

The dielectric constant measured at room temperature reaches a plateau in low frequencies (0.1 Hz – 100 Hz) and its value is 2.8. The electric breakdown for Elastosil 2030 with this thickness (160 µm), at room temperature is set to 80 MV.m^{-1} **[4]**. Fig. 6 underlines the operating area for the silicone Elastosil 2030 in conjugated plots, for a maximal applied strain of 50 %.

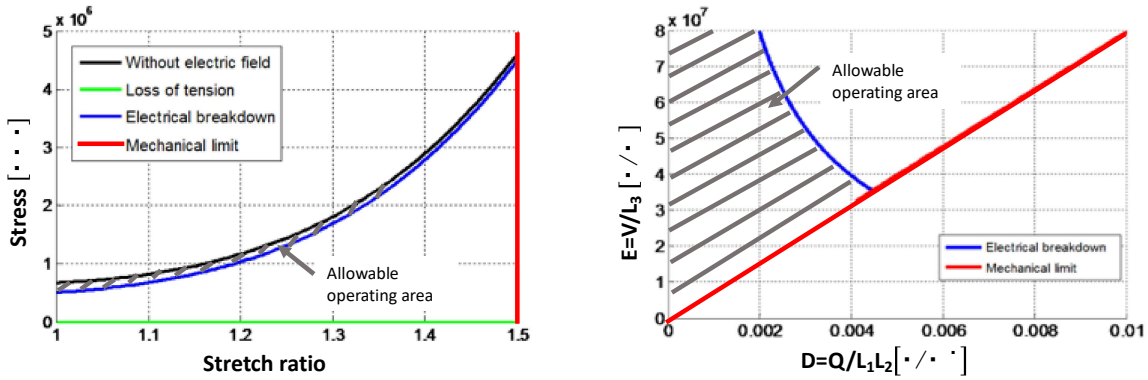

Figure 6: Thermodynamic modelling and operating area of Elastosil 2030 in conjugated plots. *E* stands for the electric field, *D* for the electric displacement, *V* is the voltage and *Q* the charge. L_1, L_2 and L_3 refer to the dimensions of the sample in the three directions.

In a biaxial mode, the silicone Elastosil 2030 does not suffer electromechanical instability known as pull-in instability. This silicone elastomer could in theory scavenge up to 0.44 J.g^{-1} under a maximal strain of 300 %, and up to 0.13 J.g^{-1} for a strain of 50 %. In comparison, we showed in **[7]** that the 3M VHB4910 acrylic polymer could scavenge in theory up to 0.834 J.g^{-1} under a maximal biaxial strain of 300 % and only 0.03 J.g^{-1} for an applied strain of 50 % without applied pre-strain. With a biaxial pre-strain of 300% x 300%, the predicted maximum scavenged energy density grow up to 0.9 J.g^{-1} for an applied strain of 50%.

A Performance Index (*PI*) must be defined in order to compare various polymers for an energy scavenging application (Eq. 12).

$$PI = E_{rec} N_f \tag{12}$$

with E_{rec} the maximum predicted scavenged energy per cycle computed thanks to our thermodynamic modelling for 1g of dielectric elastomer.

This Performance Index *PI* is basically the total energy that the dielectric elastomer will be able to scavenge during its entire life. One can underline that a more realistic prediction could be done if the electromechanical lifetime N_{em} is used instead of the mechanical lifetime N_f. N_{em} is the number of

cycles done before a failure (electric or mechanic) occurring into the dielectric elastomer when this latter one is subjected to mechanical and electrical solicitations as the one done in real applications. Nevertheless, this *PI* remains a first practical index to start comparison between materials. According to Fan *et al.* **[20]**, 18 10^4 cycles are theoretically achievable for the 3MVHB under a strain of 100 % and only 102 for a strain of 300%. Kornbluh *et al.* realized various lifetime experiments on pre-stressed 3M VHB4910 polymer under various configurations: 1 millions of cycle can be achieved with a 300% x 300% pre-stressed sample **[27]**. Thus, for 1g of active material, the *PI* is about 0.9 10^6 J for the 300% x 300% pre-stressed 3M VHB4910 under an applied active strain of 50% and about 2.21 10^6 J for the silicone Elastosil under an applied strain of 50%. This first comparison underlines that the Elastosil polymer can scavenge less energy than the 3M polymer but develops a higher fatigue life leading to a higher total scavenged energy: scavenging less energy per cycles but be able to realize millions and millions of cycles seems to be a promising approach for energy scavenging applications. The final choice of material for energy scavenging applications is clearly the combination of fatigue life and scavenged energy density rather than only one of these two parameters.

4. Conclusion

We presented a prediction of fatigue life of silicone dielectric elastomer (Elastosil 2030) using the theory of the crack growth: 17.3 millions of cycles are achievable under 50% of strain. We highlight that the power laws have a tremendous impact on the estimation of fatigue life. The specimen configuration (edge cut or pure shear) and the mechanical quantities (tearing energy and elastic energy) have less influence. Prediction of fatigue life based on crack growth approach leads rather to a range of feasible cycles, which remains an important indicator in real applications such as energy scavenging applications. Crack growth approach is a very fast and powerful test method that we will be compared in our future work to classic S-N tests under operation, for fully validation of this methodology. Finally, performance index is defined to compared various polymers for energy scavenging applications.

Acknowledgments
The authors thankfully acknowledge the financial support from the French research agency ANR through the project ANR-2014-SEASEA. C. Jean-Mistral would like to acknowledge P. Chaudet and P. Valverde for the technical support during the mechanical experiments.

References :

[1] R. Pelrine, R. Kornbluh, J. Eckerle, P. Jeuck, S. Oh, Q. Pei, Dielectric elastomers: Generator mode fundamentals and application, Proc. SPIE 4329, 148-156 (2001) https://doi.org/10.1117/12.432640

[2] P. Jean, A. Wattez, G. Ardoise, C. Melis, R. Van Kessel, A. Fourmon, E. Barrabino, J. Heemskerk, J.P. Queau, Standing wave tube electro active polymer wave energy converter, Proc. SPIE 8340, 83400C (2012) https://doi.org/10.1117/12.934222

[3] C. Jean-Mistral, J.J. Chaillout, S. Basrour , Dielectric polymer: scavenging energy from human motion *Proc. SPIE* **6927** 692716 (2008) https://doi.org/10.1117/12.776879

[4] T. Vu Cong, C. Jean-Mistral, A. Sylvestre, Electrets substituting external bias voltage in dielectric elastomer generators: application to human motion, Smart Mater. Struct. 22, 025012 (2013) https://doi.org/10.1088/0964-1726/22/2/025012

[5] A. T. Mathew, C. Liu, T. Y. N. Ng, S. J. A. Koh, A high energy dielectric-elastomer-amplified piezoelectric (DEAmP) to harvest low frequency motions, Sensors and Actuators A 294, 61–72 (2019) https://doi.org/10.1016/j.sna.2019.05.015

[6] G. Moretti, G. P. R. Papini, L. Daniele, D. Forehand, D. Ingram, R. Vertechy, M. Fontana, Modelling and testing of a wave energy converter based on dielectric elastomer generators, Proc.R.Soc.A 475: 20180566 (2019) http://dx.doi.org/10.1098/rspa.2018.0566

[7] T. Vu-Cong, C. Jean-Mistral, A. Sylvestre, New operating limits for applications with electroactive elastomer: effect of the drift of the dielectric permittivity and the electrical breakdown, Proc. SPIE 8687, 86871S (2013) https://doi.org/10.1117/12.2007698

[8] F. B. Madsen, A. E. Daugaard, S. Hvilsted, A. L. Skov, The Current State of Silicone-Based Dielectric Elastomer Transducers, Macromolecular Rapid Com. 37, 5 378-413 (2016) https://doi.org/10.1002/marc.201500576

[9] S. Park, K. Mondal, R.M. Treadway, V. Kumar, S. Ma, J.D. Holbery, M. D. Dickey, Silicones for stretchable and durable soft devices: beyond Sylgard-184, Appl. Mater. Interfaces 10, 11261-11268 (2018) https://doi.or/10.1021/acsami.7b18394

[10] Z. Suo, Theory of Dielectric Elastomers, Acta Mechanica Solida Sinica 23, 6 (2010)

[11] C.C. Foo, S. J. A. Koh, C. Keplinger, R. kaltseis, S. Bauer, Z. Suo, Performance of dissipative dielectric elastomer generatorsJ. of App. Phys. 111, 094107 (2012) http://dx.doi.org/10.1063/1.4714557

[12] J. Zhou, L; Jiang, R.E. Khayat, Investigation on the performance of a viscoelastic dielectric elastomer membrane generator, Soft Matt. 15 (2015) https://doi.org/10.1039/c5sm00036

[13] J. Zhou, L. Jiang, Development of a predictor for fatigue crack nucleation of dielectric viscoelastomers under electromechanical loads, J. of the Mech. and Phys. and Solids 119, 400-416 (2018) https://doi.org/10.1016/j.jmps.2018.07.012

[14] L. Agostini, C. Yi, M. Fontana, R. Vertechy, Lifetime performances of silicone-based dielectric elastomer transducers under cyclical electric-stress loading, Proc. EuroEAP (2018)

[15] C.A. de Saint-Aubin, S. Rosset, S. Schlatter, H. Shea, High-cycle electromechanical aging of dielectric elastomer actiators with carbon-based electrodes, Smart. Mater. Struc. 27, 074002 (2018) https://doi.org/10.1088/1361-665X/aa9f45

[16] A.N. Gent, PB. Lindley, A.G. Thomas, Cut growth and fatigue of rubbers.I. The relationship between cut growth and fatigue, J. Appl. Polym. Sci. 8, 455-466 (1964) https://doi.org/10.1002/app.1964.070080129

[17] T. Zarrin-Ghalami, A. Fatemi, Material Deformation and fatigue behaviour characterization for elastomeric component life predictions, Polymer Engineering and Science, 12, 8, 1795-1805 (2012), https://doi.org/10.1002/pen.23125

[18] W. V. Mars, A. Fatemi, A literature survey on fatigue analysis approaches for rubber, Int. J. on Fatigue 24, 949-961 (2002) https://doi.org/10.1016/S0142-1123(02)00008-7

[19] R. J. Harbour, A. Fatemi, W. V. Mars, Fatigue life analysis and predictions for NR and SBR under variable amplitude and multiaxial loading conditions, Int. J. Fatigue 30 1231–1247 (2008), doi:10.1016/j.ijfatigue.2007.08.015

[20] W. Fan, Y. Wang, S; Cai, Fatigue fracture of a highly stretchable acrylic elastomer, Polym. Test. 61, 373-377 (2017) http://dx.doi.org/10.1016/j.polymertesting.2017.06.005

[21] R.S. Rivlin, A.G. Thomas, Rupture of rubber. I. Characteristic energy for tearing, J. Polym. Sci. 10, 291-318 (1953) https://doi.org/10.1002/pol.1953.120100303

[22] M. Pharr, Y.J. Sun, Z. Suo, Rupture of highly stretchable acrylic dielectric elastomer, J. Appl. Phys. 111 (2012) https://doi.org/10.1063/1.4721777

[23] R. Kaltseis, C. Keplinger, A.S.J. Koh, R. Baumgartner, Y.F. Goh, W.H. Ng, A. Kogler, A. Tröls, C.C. Foo, Z. Suo, S. Bauer, Natural rubber for sustainable high-power electrical energy conversion, RSC Adv. **4**, 27905-13 (2014) https://doi.org/10.1039/C4RA03090G

[24] W.V. Mars, Factors that affect the fatigue life of rubber: a literature survey, J. Rubb. Chem. and Tech., **77**, 391-412 (2004)

[25] T. Zarrin-Ghalami, Fatigue Life Prediction and Modeling of Elastomeric Components, Ph-D dissertation, U. of Toledo (2013)

[26] I. Papadopoulos, Predicting the fatigue life of elastomer components, Ph-D dissertation, U. of Queen Mary-London (2005)

[27] R. Kornbluh, A. Wong-Foy, R. Pelrine, H. Prahlad, Long-lifetime all-polymer artificial muscle transducers B. Mc Coy, Proc Mater. Res. Soc. Symp. 1271 (2010)